ISSN: 2454-9940

INTERNATIONAL JOURNAL OF APPLIED SCIENCE ENGINEERING AND MANAGEMENT

E-Mail :
editor.ijasem@gmail.com
editor@ijasem.org

www.ijasem.org

INTERNATIONAL JOURNAL OF APPLIED SCIENCE ENGINEERING AND MANAGEMENT

ISSN 2454-9940

www.ijasem.org

Vol 19, Issue 2, 2025

Underwater Image Enhancement via Weighted Wavelet Visual Perception Fusion

[1] Mrs. A. Josh Mary, [2] Mrs. B. Mounika, [3] Mallireddy Ramyasri,[4]Ainavilli Satya Veni, [5]Ch.Naga Padma Manju Anusha,

[1] Associate Professor,Dept.of CSE, Rajamahendri Institute of Engineering & Technology, Bhoopalapatnam, Near Pidimgoyyi,Rajahmundry,E.G.Dist.A.P. 533107.

[2] Assistant Professor,Dept.of CSE, Rajamahendri Institute of Engineering & Technology, Bhoopalapatnam, Near Pidimgoyyi,Rajahmundry,E.G.Dist.A.P. 533107.

[3,4,5] Students,Dept.of CSE, Rajamahendri Institute of Engineering & Technology, Bhoopalapatnam, Near Pidimgoyyi,Rajahmundry,E.G.Dist.A.P. 533107.

Abstract—

Underwater images typically suffer from various quality degradation issues due to the scattering and absorption of light, but these degraded-quality underwater images are unbeneficial for analysis and applications. To effectively solve these quality degradation issues, an underwater image enhancement method via weighted wavelet visual perception fusion is introduced, called WWPF. Concretely, we first present an attenuation-map-guided color correction strategy to correct the color distortion of an underwater image. Subsequently, we employ the maximum information entropy optimized global contrast strategy to the color-corrected image to obtain a global contrast-enhanced image. Meanwhile, we apply a fast integration optimized local contrast strategy to the color-corrected image to get a local contrast-enhanced image. To exploit the complementary of the global contrast-enhanced image and the local contrast-enhanced image, we introduce a weighted wavelet visual perception fusion strategy to obtain a high-quality underwater image by fusing the high-frequency and low-frequency components of images at different scales. Our extensive experiments on three benchmarks validate that our WWPF outperforms the state-of-the-art methods in qualitative and quantitative. Besides, the underwater images processed by our WWPF also benefit practical underwater applications.

I. INTRODUCTION

The ocean, which occupies 71% of the planet, is crucial to human existence and industry. Also, it's a vital cog in the wheel of life on Earth. undersea pictures are a crucial means of conveying information about the undersea environment and making use of it in marine resource development and use [1]. The complex physical environment underwater, however, severely degrades underwater photos [2]. One the one hand, underwater photos may quickly become color cast, poor contrast, and brightly lit due to light absorption [3]. In contrast, issues like underwater picture noise amplification, detail loss, and fog blur are readily caused by light scattering [4]. In addition to posing problems for image processing and analysis, low-quality underwater photographs have a profound effect on how humans perceive the world. Consequently, there is an immediate need to address the scientific question of how to improve the clarity of underwater images. There are now three main types of underwater picture improvement approaches: image restoration, image enhancement using deep learning, and deep learning methods overall [5, 6]. To restore crisp underwater photos, early image restoration algorithms depended on certain priors. But there are a lot of priors that make these approaches less successful and less resilient [7]. Image enhancement-based approaches, in contrast to image restoration methods, do not take priors into account while adjusting pixel values to boost underwater pictures' contrast and brightness. Regrettably, they have a tendency to make the enhanced photographs seem too boosted or oversaturated [8], [9]. As a result of the abundance of training data, deep learning techniques have recently found their way into underwater picture improvement [10], [11], [12], [13]. Notably, deep learning approaches are hindered by

INTERNATIONAL JOURNAL OF APPLIED SCIENCE ENGINEERING AND MANAGEMENT
ISSN 2454-9940
www.ijasem.org
Vol 19, Issue 2, 2025

the difficulty in obtaining high-quality, large-scale, paired underwater photos. At the same time, deep learning approaches are prone to unsteady performance in the complex and ever-changing undersea environment. In conclusion, it is beneficial to study how to combine the benefits of various approaches to boost the performance and quality of underwater photos. As part of our research, we presented WWPF, an approach to underwater picture enhancement using Weighted Wavelet visual Perception Fusion. In contrast to previous fusion methods [9], [16], our

(a) (b) (c) (d) (e) (f) (g) (h) (i)

Fig. 1. **Enhanced results (bottom) of our WWPF for several raw images (top).** (a) and (b) are derived from the UCCS [14]. (c) and (d) are derived from the UIQS [14]. (e) and (f) are derived from the UIEB [15]. (g), (h), and (i) are derived from the Internet. Without fine-tuning the parameters, our WWPF obtained satisfactory visual results for different degraded images from different datasets.

WWPE employs distinct scales of high- and low-frequency components instead of different scales of weight maps in fusion techniques to incorporate the complementing benefits of different improved versions of pictures. Our WWPF is structured around three main phases that aim to improve underwater pictures' color, global and local contrast, and visual perception: attenuation-map-guided color correction, global and local contrast enhancement, and weighted wavelet visual perception fusion. The first step is to create a color transfer picture by compensating the other three color channels. We do this by redefining the various color channels and using the luminance channel as the reference channel. At the same time, in order to get a color-corrected picture, we fuse the input and color transfer pictures using an attenuation map. Next, we take the color-corrected picture and apply two strategies to improve the contrast: one is the rapid integration optimized local contrast strategy, and the other is the maximum information entropy optimized global contrast strategy. The result is an upgraded image with better contrast both globally and locally. Finally, we use a wavelet decomposition technique to extract varying-scale high- and low-frequency components from the global and local contrast-enhanced pictures. At the same time, we recreate a high-quality underwater picture by integrating multiple levels of components with varied scales using the weighted wavelet perception fusion approach. Furthermore, Fig. 1 showcases the improved outcomes of our WWPF on many deteriorated photographs. • To fix the color cast of underwater images, we present an attenuation-map-guided color correction method. This method takes into account both the fact that different levels of light attenuation cause different color distortions and the grey-scale assumption that the average grey values of each color channel remain the same before attenuation. • To enhance the color-corrected image's global contrast, we suggest an approach that maximizes information entropy; to do the same for the local contrast, we recommend a strategy that optimizes quick integration. We discovered that underwater photos may be significantly improved by combining global and local contrast-enhanced images, which have complementary but beneficial qualities. • A weighted wavelet visual perception fusion approach is introduced. This method use the wavelet decomposition technique to extract the high-frequency components from both the global and local contrast-enhanced pictures, as well as the estimated low-frequency component. Then, to recreate a top-notch underwater picture, we use the weighted inverse wavelet transform technique, which takes use of various level components with varying sizes. This section provides an overview of the paper's organization and content. Underwater image enhancement research is detailed in Section II. Each stage of our WWPF method's workflow is detailed in Section III. Section IV presents a detailed overview of the experimental data and analysis. We conclude with a brief overview and an outlook on our work in progress.

II. RELATED WORK

Image restoration, image enhancement, and deep learning approaches are the three primary categories into which underwater picture improvement techniques are currently classified. References [17], [18], and [19] are applicable. What follows is a synopsis of the present study. Methods for restoring damaged photos by inverting the degradation process and using priors to estimate underwater imaging parameters have been reported [20], [21]. Due to the comparable deterioration characteristics of underwater and foggy pictures, the dark channel prior (DCP) has recently been used to underwater image restoration with success [22], [23], [24]. Primors such as general dark channel prior [25], attenuation curve prior [26], submerged dark channel prior [27], statistical prior [28], hazy lines prior [29], and so on are the key components of these contexts. To estimate more precise transmission maps, Wang et al. [26] used statistical analysis of clear pictures' pixel distribution in RGB space and suggested an adaptive fading curve; nonetheless, the model's sensitive robustness was a result of the difficult optimization procedure. The defog method developed by Berman et al. [29] included estimating two extra global factors based on various water type spectral profiles. This method was able to fix color distortion and bring back the 3D structure of underwater sceneries, but it was somewhat time-consuming. In a complex series of processing processes, Muniraj et al. [30] calculated the transmission map's depth by comparing the channel intensities. In order to restore low-quality pictures, Liang et al. [31] presented a generalized imaging model that used an image decomposition objective function that included numerous priors, such as the grey-scale world. There is room for improvement in the performance of single-priori hypothesis approaches, nevertheless, since these methods depend on certain priors. Parameter optimization is a challenge for numerous priori approaches. Underwater photos may have their color, contrast, and clarity bumped up with the use of picture enhancement techniques.

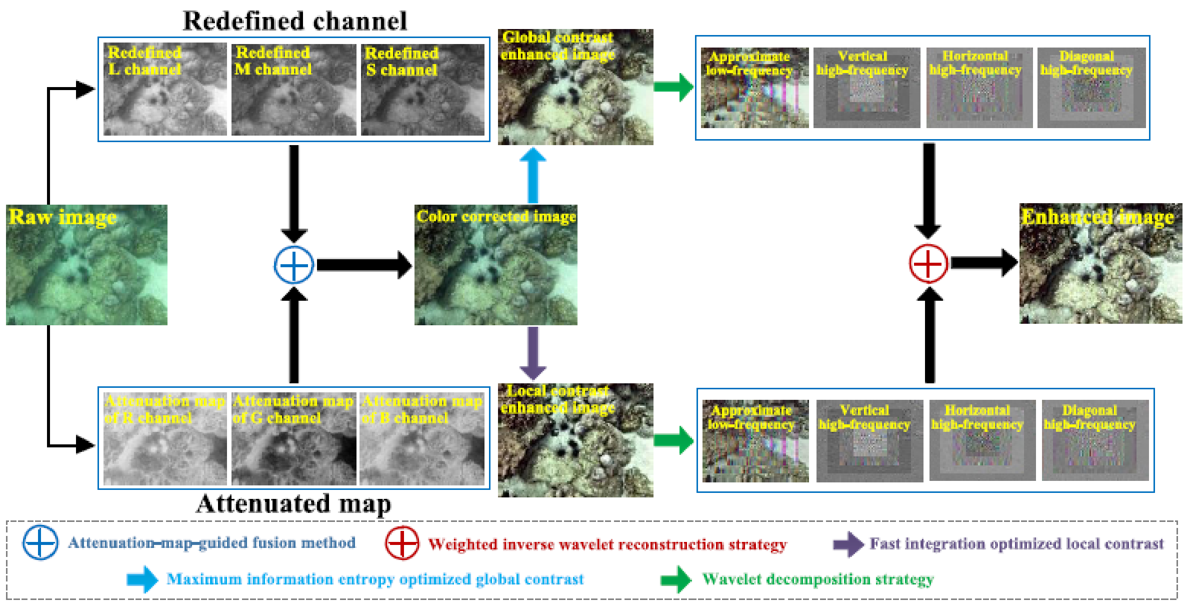

Fig. 2. **Flowchart of our proposed WWPF method.** Given a raw underwater image, it first participates in an attenuation-map-guided color correction stage to produce a color-corrected underwater image. Afterward, two images are denoted as the global contrast-enhanced and the local contrast-enhanced images. They are derived from the color-corrected image obtained by the maximum information entropy optimized global contrast method and the fast integration optimized local contrast method. Finally, the two enhanced versions of the approximate low-frequency component, vertical, horizontal, and diagonal high-frequency components, are used to reconstruct a high-quality underwater image.

an image's pixel value, as shown by the Retinex [32], [33], [34], histogram [35], [36], [37], and fusion techniques [16], [38], [39], [40], [41]. An example of a technique that over-enhanced underwater photos is the one presented by Zhang et al. [9] for color correction and detail-preserved fusion, which is based on Retinex. In their study, Zhuang et al. [32] presented a variational Retinex approach that improved underwater picture contrast and texture details while introducing micro-red distortion. The method was based on the benefits of L1/2 norm and L2 norm. To avoid the problems of under-and over-enhancement that plagued early histogram applications, Chani et al. [35] suggested a recursive adaptive histogram modification approach. The benefits of both contrast-enhanced and detail-sharpened images may be combined in a color balancing and fusion approach suggested by Ancuti et al. [16]. Based on earlier fusion work [16], Jiang et al. [39] developed a local structural batch decomposition method; however, this method fails to account for halo effects since it does not take non-uniform illumination into account. All things considered, they don't take much into account about the picture itself, therefore they can't fix issues like halo effects and color distortion in underwater photos. Convolutional Neural Networks (CNNs) and Generative Adversarial Networks (GANs) are examples of deep learning techniques that attempt to automatically extract representation characteristics from training data and create a nonlinear mapping relationship [42], [43], [44]. The application of deep learning approaches to low-level visual tasks is being done progressively, depending on the availability of training data and powerful computer systems [45, 46, 47, 48]. Li et al. [15] built an underwater enhanced dataset with pairs of high-quality and low-quality underwater photos to address the data gap. They suggested a WaterNet to validate the dataset's improved performance, drawing inspiration from CNN [49], [50]. To build synthetic underwater pictures, Li et al. [51] suggested an underwater enhancement CNN that was influenced by underwater

scenes before and used the water kinds and deterioration levels. Recent work by Zhao et al. [52] builds on prior work by CNN [51] to develop a low-weight cascade network that takes complexity and performance into account while improving underwater images. Based on GAN [53], [54], [55], Skinner et al. [56] used the underwater physical model to create synthetic underwater pictures for GAN training; nevertheless, these images do not faithfully depict the actual underwater environments. In order to improve underwater photographs collaboratively, Qi et al. [57] used corrected feature matching in conjunction with connection learning.
A goal-guided twin GAN with an edge-holding closed-loop adversarial improvement and a task-aware feedback module was created by Liu et al. [58], however, the model's complexity was raised due to the excessive number of learning techniques. While this approach does help with underwater picture quality in general, it does need a significant quantity of high-quality underwater photographs for the training phase.

III. METHODOLOGY

Figure 2 shows the flow diagram for the visual perception fusion using weighted wavelets. We acquire the two inputs for our framework using a wavelet fusion, which is based on a color-corrected version of a raw underwater picture that has had its global and local contrast enhanced. Color retouching, local and global contrast improvement, and weighted wavelet fusion are the three primary components of our approach. The first step in correcting underwater photos' distorted colors is using an attenuation map-guided fusion to eliminate the water's wavelength-dependent color absorption. This leads to a mutually beneficial interaction between the color-corrected picture and its local and global contrast-enhanced counterparts. To make a top-notch underwater picture, weighted wavelets combine these two improved versions with varying degrees of supplementary data. Following this, we will go over several methods for making underwater photos seem more detailed and with more contrast.
Part A. What Drives People Underwater photographs, in contrast to surface photos, often include a wide range of color distortions (blue, green, yellow, blue-green, etc.) caused by severe imaging and illumination restrictions. Underwater photographs and their future uses are severely impacted by these color cast difficulties, which is a major bummer. Color correction is therefore an important part of underwater picture enhancement pre-processing. To enhance underwater photographs' contrast and texture detail, color correcting isn't enough. The methods that follow will focus on improving the underwater image's contrast and detail in order to achieve this goal.
Why Color Correction Is Necessary: In recent times, color correction techniques for underwater photos have shown promise, such as statistical-based color correction [32] and piecewise color correction [59]. Nevertheless, as a result of overcorrection, these techniques do impart some reddish casts. At the same time, color channel compensation algorithms have a favorable impact on underwater picture color correction [16], [38], [60]. Color transfer techniques have been effectively used to adjust underwater photos' colors [37], [61] in order to deal with the difficulties. In order to make the most of the piecewise color correction and color channel compensation approaches, our work makes use of the color transfer method. Second, the Reasons Behind Contrast Enhancement: Underwater photographs may have their contrast and brightness improved using histogram equalization techniques [19], [62], but these approaches have the drawback of being prone to over-enhancement. These issues are reduced by using bi-histogram equalization techniques [17], [36], but, although the bi-histogram does a good job of improving the pictures' global contrast, it also makes the noise worse. The complete use of local blocks has shown notable benefits in terms of local contrast augmentation for underwater pictures [9], [37]. In order to get a high-quality underwater picture, fusion-based approaches have recently used the many feature maps to successfully combine distinct improved versions [35], [37]. To get a high-quality underwater picture, we use a weighted wavelet fusion technique, which combines the high- and low-frequency parts of the many improved versions, unlike these fusion approaches.
B. Map of Attenuation Color Correcting Using a Guide Each picture channel follows the same grayscale distribution and mean before attenuation, drawing inspiration from the grayscale world hypothesis [16]. Color overcorrection occurs in the conventional greyscale world because the constituent channels of an underwater picture are muted to different degrees. The luminance channel, often called the reference channel, is renamed to reflect the channel with the highest pixel intensity. The luminance channel's computation procedure is mathematically specified as:

$$I_l(i, j) = \max\{I_r(i, j), I_g(i, j), I_b(i, j)\}, \qquad (1)$$

where the brightness channel is Il, the red channel is Ir, the yellow channel is Ig, and the blue channel is Ib. After that, because water absorbs light, we use the luminance channel as a reference to make up for the red, green, and blue color channels' attenuation. Put another way, we may say that the average pixel intensity for each color channel is:

$$\overline{I}_c = \frac{1}{H \times W} \sum_{i=1}^{H} \sum_{j=1}^{W} I_c(i, j), \quad c \in \{l, r, g, b\}, \quad (2)$$

where W is the height and H is the breadth of each input channel. The luminance, red, green, and blue channels' mean values are I l, I r, I g, and I b, respectively. Afterwards, using the luminance channel's mean value as a reference, we may adjust the red, green, and blue channels as follows:

$$\begin{cases} I_r^C(i, j) = I_r(i, j) + (\overline{I}_l - \overline{I}_r) \times I_l(i, j) \\ I_g^C(i, j) = I_g(i, j) + (\overline{I}_l - \overline{I}_g) \times I_l(i, j) \\ I_b^C(i, j) = I_b(i, j) + (\overline{I}_l - \overline{I}_b) \times I_l(i, j), \end{cases} \quad (3)$$

where I C r, I C g, and I C b are the adjusted color channels for red, green, and blue, respectively. The histogram distribution does not hold true even if the underwater picture satisfies the grey-scale world assumption that all channels have almost equal mean grey values thanks to the aforementioned correction technique. To make each channel's dynamic range even wider, meeting the grey-scale world assumption that their histogram distributions are identical. To fix the color-transfer image—also known as the color-compensated underwater image—we use a linear stretching approach. The procedure of linear stretching is described as:

$$I_c^{CR} = I_o^{\min} + (I_c^C - I_c^{\min}) \times \frac{I_o^{\max} - I_o^{\min}}{I_c^{\max} - I_c^{\min}}, \quad c \in \{r, g, b\}, \quad (4)$$

where I CR c is the color channel that corresponds to the cth color and is used for correction. I max c is the highest possible pixel value for the cth input channel, while I min c is the lowest possible pixel value. The maximum and lowest stretching ranges for each color channel are I max o and I min o, respectively, and they are set to 0 to 255. Underwater images' wavelength-dependent light absorption effect cannot be well captured by the grey-scale world assumption, which just considers the average grey values and histogram distribution of the different color channels. Using only the color adjustment approach, the results for blue, green, and yellow underwater are shown in Fig. 3.

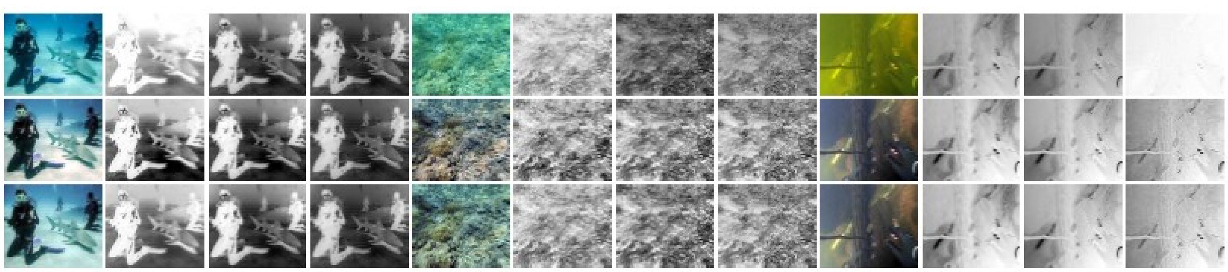

(a) (b) (c) (d) (e) (f) (g) (h) (i) (j) (k) (l)

Fig. 3. **Comparison results were yielded using the color compensation and attenuation-map-guided fusion.** From top to bottom: (a), (e), and (i) are the raw underwater images (From left to right are blue, green, and yellow underwater images.), the result of color compensation, and the result of attenuation map-guided fusion, respectively. (b), (f), and (j) are the attenuation map of the red channel, respectively. (c), (g), and (k) are the attenuation map of the green channel, respectively. (d), (h), and (l) are the attenuation map of the blue channel, respectively.

photographs experience over-correction, somewhat cyan, and slightly magenta hues. Hence, in order to acquire a color-corrected underwater picture, we make full use of the attenuation of various lights and use the attenuation map to direct the merging of the raw underwater image and the color transfer image. The maximum attenuation map is used as the guiding fusion picture to make sure that the light attenuation of each color channel can be adjusted properly. The ultimate attenuation map may be expressed mathematically as:

$$I_{\max}^A = \max\{1 - I_r{}^{\gamma}, 1 - I_g{}^{\gamma}, 1 - I_b{}^{\gamma}\}, \quad (5)$$

ISSN 2454-9940
www.ijasem.org
Vol 19, Issue 2, 2025

Ancuti et al. [63] established the default value of 1.2 for γ, the parameter that governs the intensity of the received light, and I A max, the maximum attenuation map, are all variables in this context. Then, pixel-by-pixel, we get a color-corrected underwater picture by using the attenuation map to fuse the raw and color transfer underwater images:

$$I_c^{\mathrm{CC}} = I_{\max}^A I_c^{\mathrm{CR}} + (1 - I_{\max}^A) I_c, \quad c \in \{r, g, b\}, \qquad (6)$$

when it comes to underwater photos, I CC and I CR stand for color corrected and color transfer, respectively. Figure 3 shows that the suggested approach of color correction has accomplished good results in terms of color correction and three channels with comparable attenuation, but it still has issues with contrast and detail improvement. Section C. Global Contrast Optimization Using the maximum information entropy optimal global contrast technique, we strive to increase the global contrast of the color-corrected picture in this part. To forecast how detailed a picture is, one may use image entropy to determine how evenly distributed its histograms are [64]. In the field of information theory, entropy is defined mathematically as:

$$I_{\mathrm{Entropy}} = -\sum_{i=0}^{L-1} p_i \log_2 p_i, \qquad (7)$$

The input image's dynamic range ranges from 0 to L − 1, where pi is the probability of grayscale i and L is the number of grey levels. The entropy of a picture may be decreased with histogram equalization since it integrates the image's histogram data. In order to avoid losing picture detail due to grey level consolidation, we may compare the histogram's grey level consolidation against the amount of information entropy. This way, we can make sure that the image's global contrast is properly boosted. Lastly, we optimize the global contrast in the Bi-histogram using the greatest information entropy as a measure. We begin by defining the histogram data separation threshold Iht and the dynamic range separation threshold Idt, which are necessary for maximizing global contrast. Although it restricts the Bi-histogram method's applicability, the majority of existing approaches explicitly set the two thresholds equal. Due to its inefficiency in determining the optimal dynamic separation threshold, our proposed global contrast enhancement technique is based on maximum entropy optimization. In particular, the whole greyscale range is crossed by the dynamic threshold Idt. With every iteration, the technique stretches the histograms on either side of the threshold. After that, the procedure finds the information entropy of both the left and right histograms and adds them together. The best dynamic separation threshold Ibest is the point at which the highest value of the left and right information entropies are solved, and the associated separation threshold is used. According to mathematical calculations, the highest entropy that corresponds to the ideal separation threshold is given by:

$$\begin{aligned} I_{\mathrm{best}} &= \operatorname{argmax}(I_{\mathrm{Entropy}}(I_{\mathrm{ht}})), \quad I_{\mathrm{ht}} \in [0, L-1], \\ &\text{s. t. } I_{\mathrm{Entropy}}(I_{\mathrm{ht}}) = I_{\mathrm{Entropy}}^{\mathrm{Left}}(I_{\mathrm{ht}}) + I_{\mathrm{Entropy}}^{\mathrm{Right}}(I_{\mathrm{ht}}), \qquad (8) \end{aligned}$$

with I Left Entropy(Iht) standing for the information entropy of the left histogram of the optimized global contrast picture and I Right Entropy(Iht) for the right histogram. Here is how they explain their computation process:

$$\begin{aligned} I_{\mathrm{Entropy}}^{\mathrm{Left}}(I_{\mathrm{ht}}) &= -\sum_{i=0}^{I_{ht}} p_i \log_2 p_i, \\ I_{\mathrm{Entropy}}^{\mathrm{Right}}(I_{\mathrm{ht}}) &= -\sum_{i=I_{ht}+1}^{L-1} p_i \log_2 p_i, \qquad (9) \end{aligned}$$

When Iht varies, Pi is the probability of each gray level once the sub-histogram is equalized. Cooperation and mutual effect are key components of iterative optimization.

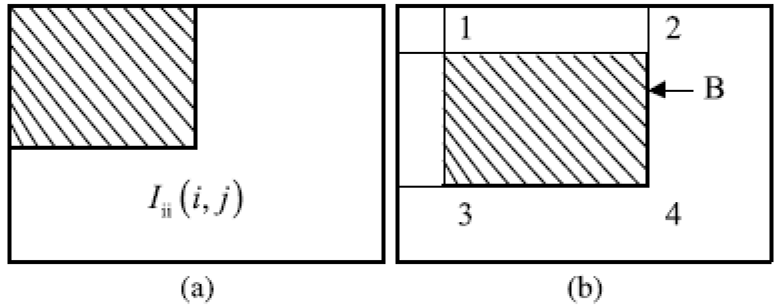

Fig. 4. (a) Example of an integral image. (b) Operation flowchart of an integral image.

of I_{ht} and I_{dt} are mainly reflected as:

$$\begin{aligned} I_{\mathrm{HE}} &= I_{\mathrm{HE}}^{\mathrm{Left}} \cup I_{\mathrm{HE}}^{\mathrm{Right}}, \\ I_{\mathrm{HE}}^{\mathrm{Left}}(T) &= (I_{\mathrm{dt}} - I_{\mathrm{min}}) \times \mathrm{CDF}(T) + I_{\mathrm{min}}, \\ & T \in [0, I_{\mathrm{ht}}], \\ I_{\mathrm{HE}}^{\mathrm{Right}}(T) &= (I_{\mathrm{max}} - I_{\mathrm{dt}}) \times \mathrm{CDF}(T) + I_{\mathrm{dt}}, \\ & T \in [I_{\mathrm{ht}} + 1, L - 1], \end{aligned} \tag{10}$$

where CDF() denotes the cumulative distribution function of the histogram and Imax and Imin stand for the maximum and lowest gray levels, respectively. The optimal dynamic range threshold Ibest is obtained by maximizing the information entropy of the complete histogram, as shown in the above solution method. By maximizing the image information entropy after histogram equalization, we are able to derive the global contrast enhanced underwater image (IGE) from the color-corrected underwater picture.

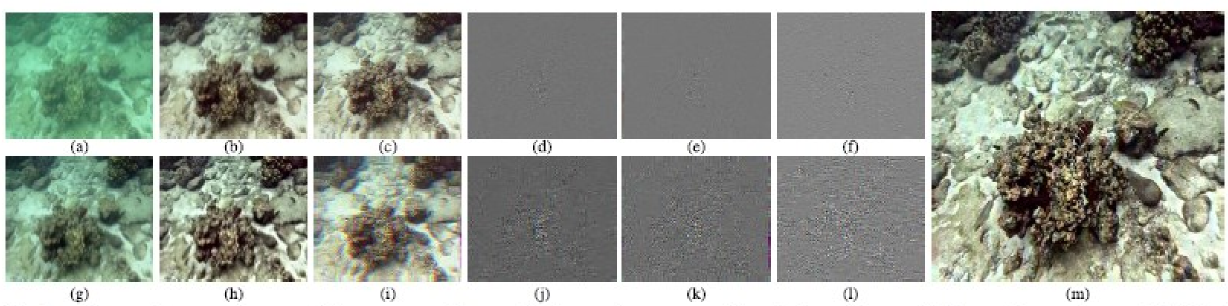

Fig. 5. **Raw underwater image and its corresponding results for each core step.** From left to right are (a) Raw underwater image, (b) Global contrast-enhanced image, (c) Approximate low-frequency component, (d) Vertical high-frequency component, (e) Horizontal high-frequency component, (f) Diagonal high-frequency component, (g) Color corrected image, (h) Local contrast-enhanced image, (i) Approximate low-frequency component, (j) Vertical high-frequency component, (k) Horizontal high-frequency component, (l) Diagonal high-frequency component, (m) Enhanced underwater image, respectively.

IV. EXPERIMENT AND ANALYSIS

Here, we assess the efficacy of our WWPF approach by conducting comprehensive quantitative and qualitative tests on a number of industry-standard datasets. Next, we look at the results of the detail augmentation, ablation experiments, application testing, and generalization performance analyses. Because of space constraints, the majority of the experimental data are included in the supplemental materials. Alternative Approaches: Our WWPF was evaluated alongside ten other approaches. These methods included three for image restoration (GDCP [26], DTVR [6], GIFM [31]), three for image enhancement (CBAF [16], BRUE [33], ADCE [38]), and four for deep learning (FUnIE-GAN [53], UIECˆ2-Net [50], PUIE-Net [55], SGUIE-Net [2]). We utilized the code1 that other writers have duplicated as CBAF [16]'s source code is not accessible to the public. We used the authors' provided programs to produce their findings for the following methods: GDCP [26], DTVR [6], GIFM [31], BRUE [33], ADCE [38], FUnIE-GAN [53], UIEC2-Net [50], PUIE-Net [55], and SGUIE-Net [2]. We have chosen three benchmark datasets—UCCS [14], UIQS [14], and UIEB [15]—to evaluate the efficacy of our WWPF approach. In order to test how well various approaches for underwater picture color correcting work, UCCS [14] is divided into three 100-image subsets: bluish, blue-green, and greenish tones. In order to compare how well various strategies improve visibility in underwater photographs, UIQS [14] uses 726-image subsets of A, B, C, D, and E degradation levels. In order to test how well various technologies improve underwater photographs, UIEB [15] compiles 890 images with varying degrees of deterioration. Criteria for Assessment: Using five widely-used metrics for evaluating image quality—average gradient (AG) [36], information entropy (IE) [64], edge intensity (EI) [36], underwater color image quality evaluation metric (UCIQE) [66], and colorfulness contrast fog density index (CCF) [67]—we quantitatively assess the enhancement performance of various methods. Image clarity is improved with a higher AG [36] score. Images with higher IE [64] scores have more detailed information. With a higher EI [36] score, the image's texture becomes more apparent. A higher CCF [67] or UCIQE [66] score indicates that human visual perception is superior. You should know that UCIQE and CCF scores don't always show how well underwater picture enhancing techniques work. A. UCCS Dataset Assessment 1) Weighing Qualitatively: The main goal for evaluating the performance of various approaches in underwater picture quality assessment is the capacity to correct color distortion. As a preliminary step, we compare how well various approaches fix colors on the UCCS dataset. The structural complexity of the undersea landscape is severely diminished by the different forms of color distortion, as seen in Figure 6 (a). Unsatisfactory color correcting performance is achieved using GDCP [26], DTVR [6], and GIFM [31]. SGUIE-Net [2], BRUE [33], CBAF [16], and FUnIE-GAN [53] all produce distorted colors that aren't desired, such reddish, yellowish, and blue artifacts. When it comes to underwater photos, UIECˆ2-Net [50], PUIE-Net [55], and ADCE [38] all do an excellent job of correcting color distortions, although ADCE lowers the saturation and detail of the improved underwater image. In comparison to our WWPF technique, UIECˆ2-Net [50] and PUIE-Net [55] perform worse when it comes to detail and contrast improvement.

To sum up, our WWPF approach is effective in enhancing contrast and texture detail and has a high ability to cure underwater photographs' many color distortion problems. 2) Quantitative Comparisons: Our WWPF approach performs well in terms of qualitative assessment when it comes to improving color, texture detail, and contrast. The benefits of our WWPF are being objectively assessed using evaluation measures at the same time. The scores of several approaches evaluated on the UCCS [14] dataset are reported in Table I using the following headings: AG [36], IE [64], EI [36], UCIQE [66], and CCF [67]. Our WWPF technique also performs well in the quantitative assessment, as shown in Table I, where it has the top or near-highest scores for AG [36], IE [64], EI [36], UCIQE [66], and CCF [67]. When applied to the UCCS dataset, our technique yields satisfactory quantitative and qualitative outcomes. B. Using the UIQS Dataset for Assessment 1) Weighing Qualitatively: We go a step further by comparing the effectiveness of several approaches to improving the clarity of underwater photos with varying degrees of deterioration using the UIQS [14] dataset. Figure 7 shows that the majority of the strategies enhance the clarity of underwater photos from UIQS that have been deteriorated [17]. When it comes to fixing color distortion, GDCP [26], DTVR [6], GIFM [31], FUnIE-GAN [53], and SGUIE-Net [2] fall short. Certain situations may see the introduction of reddish halos and local artifacts when using CBAF [16], BRUE [33], or ADCE [38]. The color correction results obtained by UIECˆ2-Net [50], PUIE-Net [55], and our WWPF are all good. When it comes to improving contrast, UIECˆ2-Net [50] and PUIE-Net [55] are stronger than GDCP [26], DTVR [6], GIFM [31], FUnIE-GAN [53], and SGUIE-Net [2]. In terms of contrast improvement, CBAF [16], BRUE [33], and ADCE [38] outperform UIECˆ2-Net [50] and PUIE-Net [55]. In contrast, ADCE [38], BRUE [33], and CBAF [16] could obliterate texture features or cause local artifacts. When compared to the aforementioned approaches, our WWPF approach successfully improves color correction, contrast improvement, and detail sharpening.

ISSN 2454-9940
www.ijasem.org
Vol 19, Issue 2, 2025
INTERNATIONAL JOURNAL OF APPLIED SCIENCE ENGINEERING AND MANAGEMENT

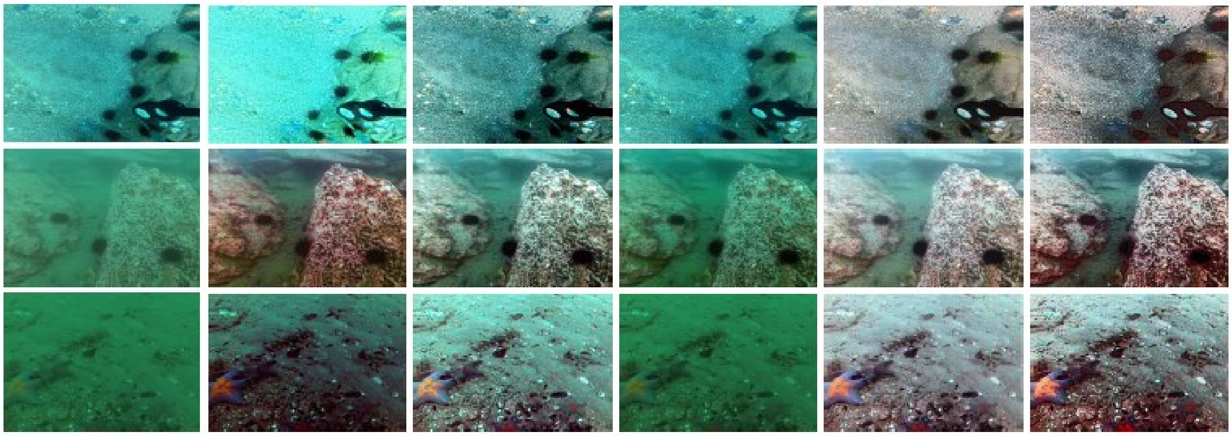

(a) Raw image (b) GDCP [26] (c) DTVR [6] (d) GIFM [31] (e) CBAF [16] (f) BRUE [33]

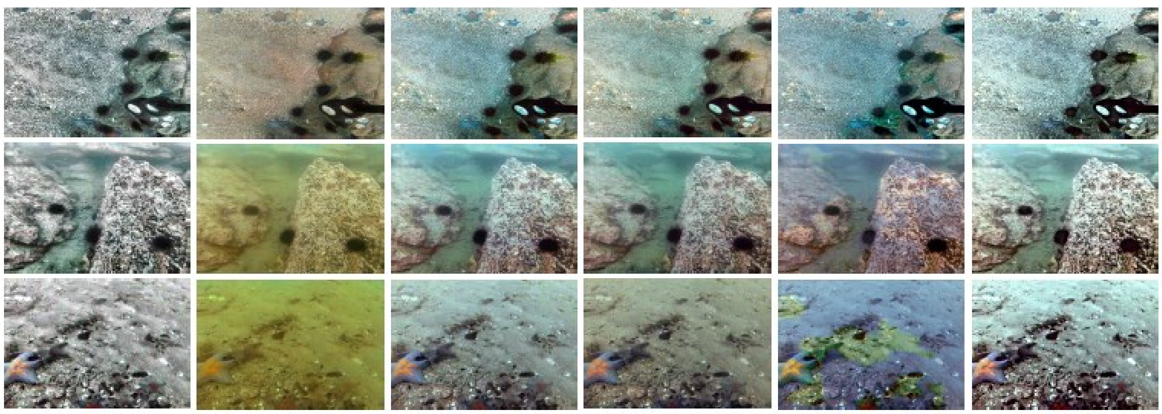

(g) ADCE [38] (h) FUnIE-GAN [53] (i) UIEC^2-Net [50] (j) PUIE-Net [55] (k) SGUIE-Net [2] (l) WWPF

Fig. 6. **Visual comparisons on three underwater images with color casts sampled from the UCCS [14] dataset.** From top to bottom are samples of blue, blue-green, and green distorted underwater images.

QUANTITATIVE EVALUATION SCORES OF OUR WWPF METHOD WITH THE COMPARED METHODS TESTED ON THE UCCS [14], UIQS [14], AND UIEB [15] DATASETS. THE HIGHEST QUANTITATIVE SCORES ARE MARKED IN RED, WHILE THE SECOND-HIGHEST SCORES ARE MARKED IN BLUE

Methods	UCCS [14]					UIQS [14]					UIEB [15]					Mean
	AG↑	IE↑	EI↑	UCIQE↑	CCF↑	AG↑	IE↑	EI↑	UCIQE↑	CCF↑	AG↑	IE↑	EI↑	UCIQE↑	CCF↑	
GDCP [26]	5.604	7.158	55.549	0.540	24.821	5.732	7.145	57.687	0.540	21.805	5.604	7.158	55.549	0.540	24.821	18.684
DTVR [6]	7.547	7.660	75.368	0.583	32.956	7.917	7.545	79.930	0.592	31.717	7.547	7.660	75.368	0.608	32.956	25.064
GIFM [31]	3.583	7.334	35.991	0.494	23.624	3.916	7.352	40.728	0.524	22.407	5.119	7.426	50.635	0.567	26.621	15.755
CBAF [16]	6.564	7.632	64.990	0.580	20.746	6.721	7.596	67.332	0.582	20.683	6.564	7.632	64.990	0.580	20.746	20.263
BRUE [33]	9.886	7.783	97.087	0.585	30.360	10.090	7.755	100.51	0.594	30.643	9.886	7.783	97.087	0.593	30.360	29.400
ADCE [38]	9.276	7.668	92.337	0.527	26.976	9.394	7.652	94.917	0.528	26.814	9.276	7.668	92.337	0.527	26.976	27.525
FUnIE-GAN [53]	3.711	7.420	37.913	0.497	16.449	3.748	7.434	38.705	0.510	17.834	3.711	7.420	37.913	0.497	16.449	13.347
UIEC^2-Net [50]	5.708	7.586	56.804	0.562	19.709	6.013	7.580	60.726	0.568	20.228	5.708	7.586	56.804	0.562	19.709	18.390
PUIE-Net [55]	4.913	7.506	49.444	0.526	19.560	5.242	7.423	53.473	0.538	20.521	6.044	7.583	60.040	0.581	21.595	17.666
SGUIE-Net [2]	5.641	7.595	56.552	0.560	23.706	5.836	7.521	59.405	0.565	23.614	7.451	7.670	74.102	0.614	31.662	20.833
WWPF	9.403	7.806	93.557	0.588	34.750	9.909	7.785	99.796	0.595	36.767	10.818	7.684	105.982	0.617	40.851	31.127

2) Comparing Quantitatively: The results of several technique tests on the UIQS [14] dataset are shown in Table I, which includes the scores for AG [36], IE [64], EI [36], UCIQE [66], and CCF [67]. The quantitative examination of the complete UIQS [14] dataset shows that our WWPF approach has the best score, or very close to it, as shown in Table I. From a qualitative and quantitative standpoint, our WWPF technique outperforms the alternatives when evaluating underwater photos with varying degrees of deterioration. C. Assessment Using the UIEB Dataset 1) Weighing Qualitatively: We quantitatively compare our technique to other ways using the UIEB [15] dataset to further assess the enhancing performance of our WWPF method for various forms of underwater picture deterioration. To thoroughly test the improved performance of our WWPF approach, we used blurred, green-distorted, and blue-distorted underwater photos (Fig. 8 (a)). No amount of color correction can fix an underwater picture that is green-distorted using GDCP[26], GIFM[31], or FUnIE-GAN [53]. There are several issues with the color correction results and the introduction of local artifacts in DTVR [6], ADCE [38], and PUIE-Net [55]. While UIECˆ2-Net [50], SGUIE-Net [2], CBAF [16], and BRUE [33] are effective in correcting green distortion, they

INTERNATIONAL JOURNAL OF APPLIED SCIENCE ENGINEERING AND MANAGEMENT
ISSN 2454-9940
www.ijasem.org
Vol 19, Issue 2, 2025

all add a small red distortion. Better removal of the green distortion is achieved with our WWPF approach, and no extra

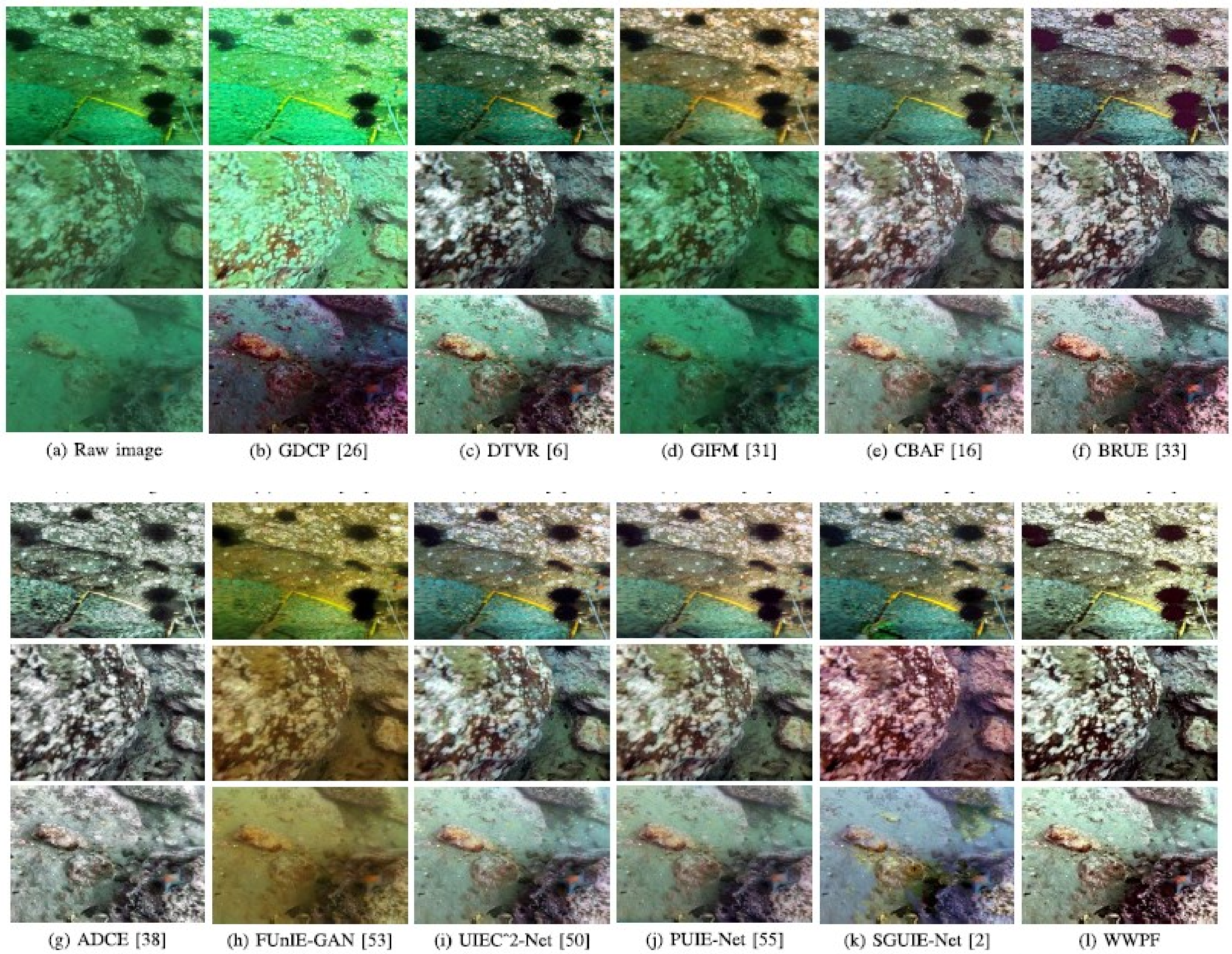

Fig. 7. **Visual comparisons on underwater images with different levels of degradation sampled from the UIQS [14] dataset.** From top to bottom are samples of underwater images with quality levels A, C, and D.

seems quite reddish. The color distortion problem is worsened for underwater images with blue distortion when using GDCP [26], DTVR [6], GIFM [31], and FUnIE-GAN [53]. No amount of tweaking can fix the blue distortion in the backdrop with CBAF [16], UIEC^2-Net [50], or PUIE-Net [55]. While BRUE [33], ADCE [38], and SGUIE-Net [2] do a decent job of correcting colors, our WWPF outperforms them when it comes to improving texture detail and contrast. The deblurring capabilities of GDCP [26], FUnIE-GAN [53], PUIE-Net [55], and SGUIE-Net [2] are inadequate for underwater images that are blurry. The deblurring effects of GIFM [31], CBAF [16], BRUE [33], and UIEC^2-Net [50] are satisfactory, but the texture details they increase are inadequate. We found that our WWPF performs better at deblurring and improving texture details compared to ADCE [38], which loses texture details, while DTVR [6] presents the overexposure issue. 2) Analyzing Data Quantitatively: Scores for AG[36], IE[64], EI[36], UCIQE[66], and CCF[67] from various methodologies evaluated on the UIEB [15] dataset are shown in Table I. According to Table I, our WWPF got the highest quantitative score, or very close to it. Our WWPF also outperforms the competition on the UCCS[14], UIQS[14], and UIEB [15] datasets in terms of total mean quantitative score. For all three benchmark datasets, our WWPF produces respectable quantitative and qualitative outcomes.

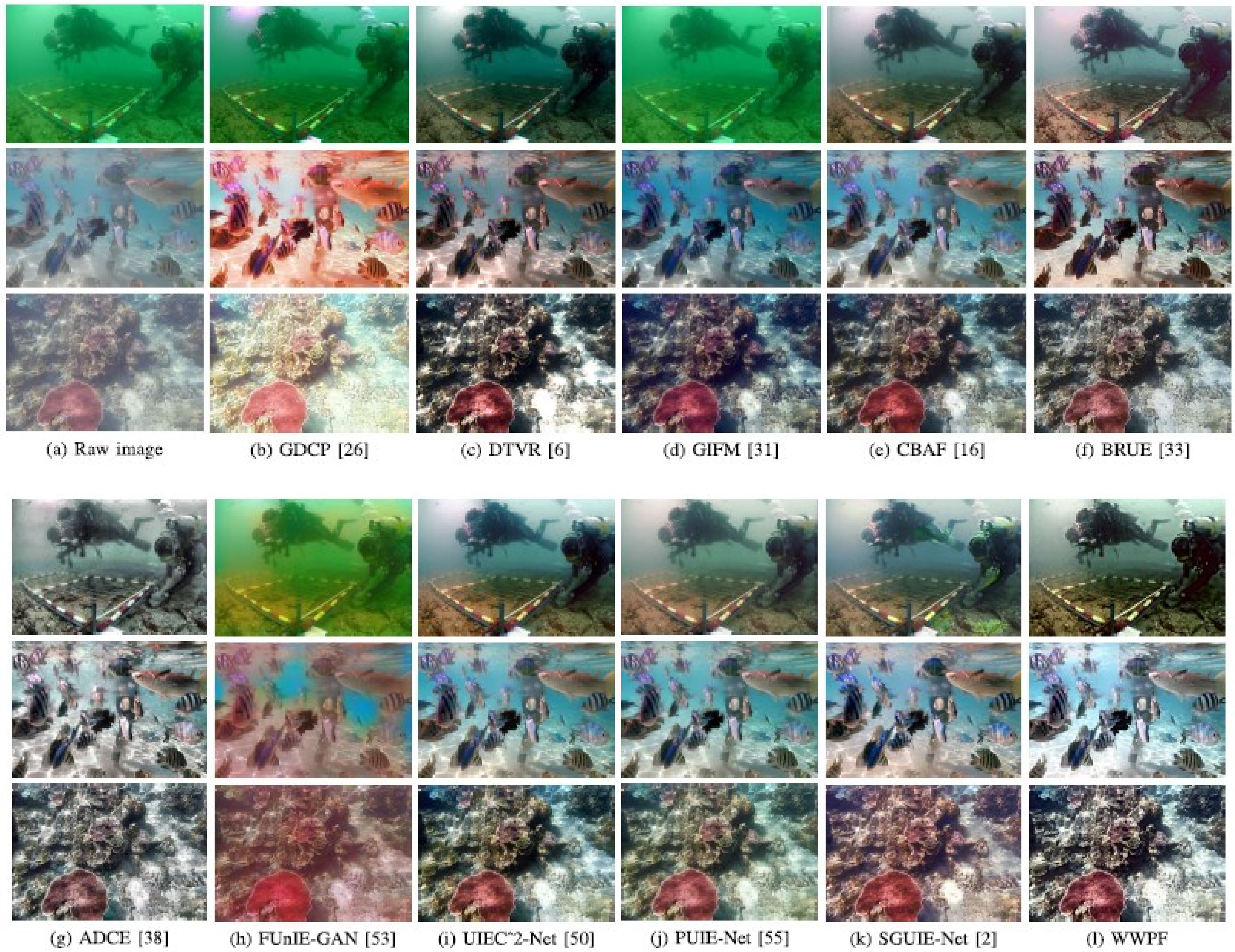

Fig. 8. **Visual comparisons on underwater images of different degradation types sampled from the UIEB dataset [15].** From top to bottom are green-distorted, blue-distorted, and blurred underwater images.

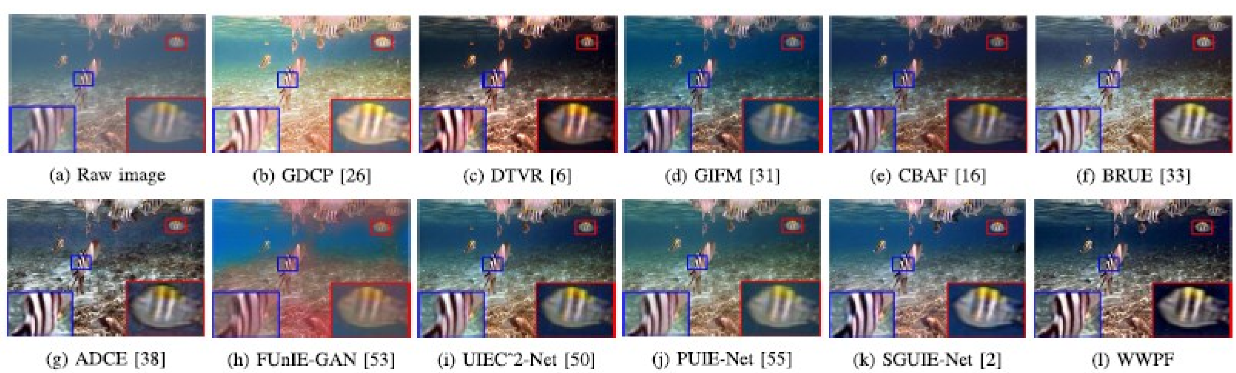

Fig. 9. **Texture detail enhancement comparisons on a typical underwater image with bluish and low visibility sampled from the UIEB [15] dataset.**

our WWPF technique unaffected by AMGCC; (b) our WWPF method unaffected by optimized global contrast; (c) our WWPF method unaffected by optimized local contrast; and (d) our WWPF method unaffected by weighted wavelet fusion. Our visual findings of evaluating the WWPF approach on the UCCS [14], UIQS [14], and UIEB [15] datasets are reported in Fig. 10. You can see the findings visually in Fig. 10. Here they are: 1) Without AMGCC, underwater images are more visible, but color correction and local contrast enhancement are not as effective. 2) Without OGC, local contrast enhancement is great, but global contrast enhancement could use some work. 3) Without

OLC, global contrast enhancement is effective, but local contrast enhancement is lacking. 4) Without WWF, fusing global and

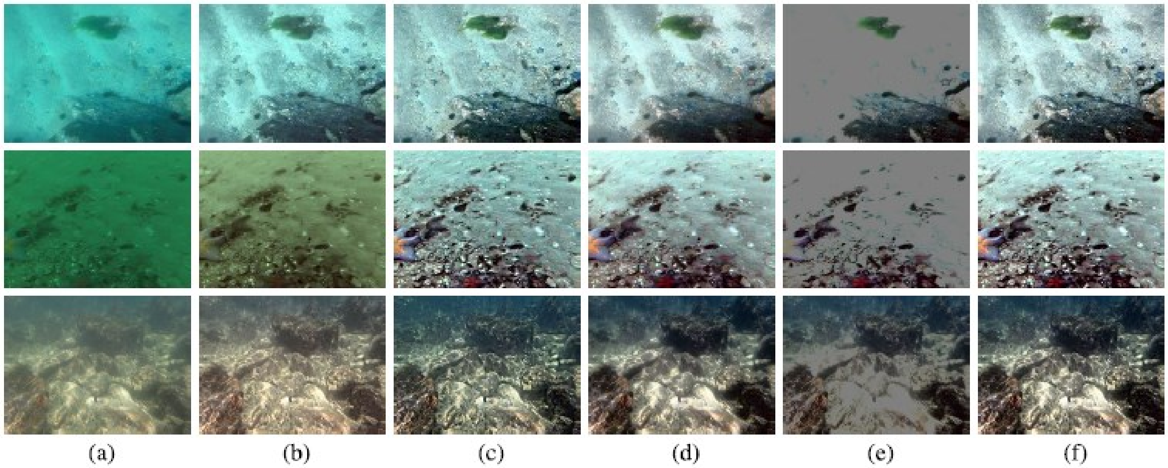

Fig. 10. **Ablation results of each core module of our WWPF method test on the UCCS [14], UIQS [14], and UIEB [15] datasets.** (a) Raw underwater images. (b) -w/o AMGCC. (c) -w/o OGC. (d) -w/o OLC. (e) -w/o WWF. (f) WWPF (full model).

TABLE II

ABLATION STUDIES OF DIFFERENT MODULES TESTED ON THE UCCS [14], UIQS [14], AND UIEB [15] DATASETS. THE HIGHEST QUANTITATIVE SCORES ARE MARKED IN RED, WHILE THE SECOND-HIGHEST SCORES ARE MARKED IN BLUE

Ablated models	UCCS [14]					UIQS [14]					UIEB [15]				
	AG↑	IE↑	EI↑	UCIQE↑	CCF↑	AG↑	IE↑	EI↑	UCIQE↑	CCF↑	AG↑	IE↑	EI↑	UCIQE↑	CCF↑
-w/o AMGCC	5.455	7.248	53.540	0.465	18.294	6.013	7.282	60.171	0.487	20.798	8.655	7.523	84.500	0.573	33.096
-w/o OGC	9.461	7.709	93.986	0.575	29.072	9.887	7.692	99.469	0.581	29.838	10.844	7.666	104.163	0.609	34.281
-w/o OLC	6.761	7.795	67.395	0.577	29.367	6.955	7.032	70.925	0.583	30.425	7.861	7.732	77.005	0.608	33.539
-w/o WWF	3.343	3.944	33.903	0.454	19.191	3.772	4.208	38.477	0.458	21.561	4.874	4.876	48.027	0.479	24.835
WWPF (full model)	9.403	7.806	93.557	0.588	34.750	9.909	7.785	99.796	0.595	36.767	10.818	7.684	105.982	0.617	40.851

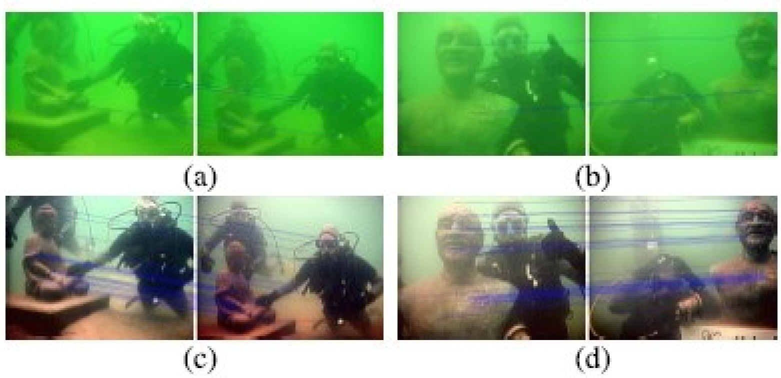

Fig. 11. **Examples of key feature point matching before and after underwater images are enhanced.** (a) and (b) represent the matching results of key feature points of the raw underwater image pairs. (c) and (d) represent the key feature point matching results of the raw underwater image pairs enhanced by our method.

ISSN 2454-9940

www.ijasem.org

Vol 19, Issue 2, 2025

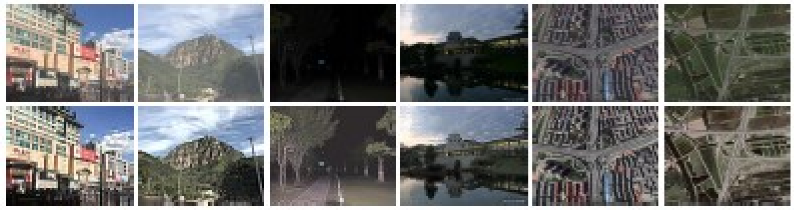

Fig. 12. **Visual results of our method for enhancing foggy, low light, and remote sensing images.** Two pairs from top to bottom are the foggy images, the images defogged by our method, the low light images, the low light images enhanced by our method, the remote sensing images, and the remote sensing enhanced by our method, respectively.

V. CONCLUSION

Here, we lay out the plan for improving underwater images. Among the primary components of our approach are weighted wavelets of various improved underwater pictures, color correction, and optimization of both global and local contrast. To compensate for the differences in global and local contrast as well as texture characteristics across pictures of various improved versions, we use weighted wavelet fusion. Our WWPF showed strong generalizability and exceptional enhancement capabilities on three benchmark datasets, according to quantitative and qualitative tests. Our WWPF does a good job of producing respectable results, however it falls short when it comes to suppressing picture noise when compared to other approaches. Accordingly, in further studies, we will investigate methods for efficient noise suppression that do not compromise the improved performance of our WWPF approach.

REFERENCES

[1] C. Fu et al., "Rethinking general underwater object detection: Datasets,challenges, and solutions," Neurocomputing, vol. 517, pp. 243–256,Jan. 2023.
[2] Q. Qi, K. Li, H. Zheng, X. Gao, G. Hou, and K. Sun, "SGUIE-Net:Semantic attention guided underwater image enhancement with multiscaleperception," IEEE Trans. Image Process., vol. 31, pp. 6816–6830,2022.
[3] H. Lu, Y. Li, T. Uemura, H. Kim, and S. Serikawa, "Low illuminationunderwater light field images reconstruction using deep convolutionalneural networks," Future Gener. Comput. Syst., vol. 82, pp. 142–148,May 2018.
[4] W. Zhang, L. Dong, T. Zhang, and W. Xu, "Enhancing underwaterimage via color correction and Bi-interval contrast enhancement," SignalProcess., Image Commun., vol. 90, Jan. 2021, Art. no. 116030.
[5] L. Chen et al., "Perceptual underwater image enhancement with deeplearning and physical priors," IEEE Trans. Circuits Syst. Video Technol.,vol. 31, no. 8, pp. 3078–3092, Aug. 2021.
[6] X. Ding, Z. Liang, Y. Wang, and X. Fu, "Depth-aware total variationregularization for underwater image dehazing," Signal Process., ImageCommun., vol. 98, Oct. 2021, Art. no. 116408.
[7] J. Xie, G. Hou, G. Wang, and Z. Pan, "A variational framework forunderwater image dehazing and deblurring," IEEE Trans. Circuits Syst.Video Technol., vol. 32, no. 6, pp. 3514–3526, Jun. 2022.
[8] H. Song, L. Chang, Z. Chen, and P. Ren, "Enhancement-Registration-Homogenization (ERH): A comprehensive underwater visual reconstructionparadigm," IEEE Trans. Pattern Anal. Mach. Intell., vol. 44, no. 10,pp. 6953–6967, Oct. 2022.
[9] W. Zhang, L. Dong, and W. Xu, "Retinex-inspired color correction anddetail preserved fusion for underwater image enhancement," Comput.Electron. Agricult., vol. 192, Jan. 2022, Art. no. 106585.
[10] H. Wang, S. Sun, and P. Ren, "Meta underwater camera: A smartprotocol for underwater image enhancement," ISPRS J. Photogramm.Remote Sens., vol. 195, pp. 462–481, Jan. 2023.
[11] C. Li, S. Anwar, J. Hou, R. Cong, C. Guo, and W. Ren, "Underwaterimage enhancement via medium transmission-guided multi-color spaceembedding," IEEE Trans. Image Process., vol. 30, pp. 4985–5000, 2021.
[12] Z. Jiang, Z. Li, S. Yang, X. Fan, and R. Liu, "Target oriented perceptualadversarial fusion network for underwater image enhancement," IEEETrans. Circuits Syst. Video Technol., vol. 32, no. 10, pp. 6584–6598,Oct. 2022.
[13] Z. Huang, J. Li, Z. Hua, and L. Fan, "Underwater image enhancementvia adaptive group attention-based multiscale cascade transformer,"IEEE Trans. Instrum. Meas., vol. 71, pp. 1–18, 2022.

[14] R. Liu, X. Fan, M. Zhu, M. Hou, and Z. Luo, "Real-world underwaterenhancement: Challenges, benchmarks, and solutions under naturallight," IEEE Trans. Circuits Syst. Video Technol., vol. 30, no. 12,pp. 4861–4875, Dec. 2020.
[15] Agrawal, K. K. ., P. . Sharma, G. . Kaur, S. . Keswani, R. . Rambabu, S. K. . Behra, K. . Tolani, and N. S. . Bhati. "Deep Learning-Enabled Image Segmentation for Precise Retinopathy Diagnosis". *International Journal of Intelligent Systems and Applications in Engineering*, vol. 12, no. 12s, Jan. 2024, pp. 567-74, https://ijisae.org/index.php/IJISAE/article/view/4541.
[16] C. Li et al., "An underwater image enhancement benchmark dataset andbeyond," IEEE Trans. Image Process., vol. 29, pp. 4376–4389, 2020.
[17] C. O. Ancuti, C. Ancuti, C. De Vleeschouwer, and P. Bekaert, "Colorbalance and fusion for underwater image enhancement," IEEE Trans.Image Process., vol. 27, no. 1, pp. 379–393, Jan. 2018.
[18] W. Zhang, X. Pan, X. Xie, L. Li, Z. Wang, and C. Han, "Color correctionand adaptive contrast enhancement for underwater image enhancement,"Comput. Electr. Eng., vol. 91, May 2021, Art. no. 106981.
[19] Q. Jiang, Y. Gu, C. Li, R. Cong, and F. Shao, "Underwater imageenhancement quality evaluation: Benchmark dataset and objectivemetric," IEEE Trans. Circuits Syst. Video Technol., vol. 32, no. 9,pp. 5959–5974, Sep. 2022.
[20] X. Fu and X. Cao, "Underwater image enhancement with global–local networks and compressed-histogram equalization," Signal Process.,Image Commun., vol. 86, Aug. 2020, Art. no. 115892.
[21] Samota, H. ., Sharma, S. ., Khan, H. ., Malathy, M. ., Singh, G. ., Surjeet, S. and Rambabu, R. . (2024) "A Novel Approach to Predicting Personality Behaviour from Social Media Data Using Deep Learning", *International Journal of Intelligent Systems and Applications in Engineering*, 12(15s), pp. 539–547. Available at: https://ijisae.org/index.php/IJISAE/article/view/4788
[22] C. Li, J. Guo, C. Guo, R. Cong, and J. Gong, "A hybrid methodfor underwater image correction," Pattern Recognit. Lett., vol. 94,pp. 62–67, Jul. 2017.